



# Assessment of Human Health Risk Caused by Heavy Metals in Kiln Dust from Coal-Fired Clay Brick Factories in Türkiye

Şeref Turhan<sup>1</sup> · Ergin Murat Altuner<sup>2</sup> · Temel K. Bakır<sup>3</sup> · Celalettin Duran<sup>4</sup> · Aybaba Hançerlioğulları<sup>1</sup> · Aslı Kurnaz<sup>1</sup>

Received: 21 April 2024 / Revised: 8 June 2024 / Accepted: 2 August 2024  
© The Author(s) 2024

## Abstract

Heavy metal (HM) pollution from natural processes and different anthropogenic activities pose significant human and environmental health risks because of their stability, non-degradable properties, and high toxicity. HM released into the air in the form of dust can enter the human body via ingestion, inhalation, and dermal contact. Keeping in mind the significance of estimating the risk from HM in different environments, the carcinogenic and non-carcinogenic health risks to workers caused by HM in kiln dust (KD) samples collected from coal-fired clay brick factories in the Western Black Sea Region of Türkiye were assessed for the first time in this study. The concentrations of major and minor oxides and HMs in the collected KD samples were analyzed using energy-dispersive X-ray fluorescence spectrometry. The average concentrations of Fe, Mn, Cr, Ni, V, Zn, Cu, As, Co and Pb analyzed in thirty-three KD samples were determined as 65444, 768, 251, 249, 248, 122, 60, 52, 42 and 16 mg/kg dw, respectively. The average levels of Ni, As, Cr, Co and Cu exceed the maximum contaminant levels recommended in the Turkish Regulation on Control of Soil Pollution. Carcinogenic and non-carcinogenic human health risk assessments for workers via three exposure pathways were carried out, estimating the hazard index (HI) and total carcinogenic risk (TCR) index, respectively. The HI values (< 1) revealed no possible non-carcinogenic health risk due to exposure to all HMs in the studied KD samples. The average TCR value revealed that the potential cancer risks for Ni, As, Cr, and Pb were slightly above the safe limit and required monitoring and further investigation for these HMs.

**Keywords** Toxic heavy metal · Kiln dust · Health assessment · Cancer risk index · Hazard index

## Introduction

Today, the word “heavy metal (HM)” has been utilized to define metallic such as vanadium (V), manganese (Mn), chromium (Cr), iron (Fe), lead (Pb), nickel (Ni), cobalt (Co), zinc (Zn), copper (Cu), etc. and metalloids such as arsenic (As), germanium (Ge), etc. chemical elements with high atomic weight or high density (approximately 5 times greater than the density of water) that are toxic to humans and the

environment (Briffa et al. 2020). HMs, which are natural constituents of the Earth’s crust, mainly exist in rocks as oxides and sulfides, (Miletić et al. 2023; Torres et al. 2023). The increase in the utilization of HMs in various commercial and industrial activities including construction, electronics, and transportation, due to world population growth and economic developments has led to a rapid increase in metallic substances in both terrestrial and aquatic environments (Briffa et al. 2020; Miletić et al. 2023). Therefore, high amounts of HM may occur in the environment owing to anthropogenic activities (foundries, mining, smelting, metal leaching, metal piping, petrochemical plants, oil refineries, traffic, coal-burning power stations, chemical industry, pesticides, insecticides, fertilizers, etc.) and natural (lithogenic) processes (geological weathering, soil erosion, acid drainage, volcanic activity, etc.) (Torres et al. 2023; Miletić et al. 2023; Yoon et al. 2023). HMs are very stable and do not biodegrade and disappear, so they can persevere in the environment for long periods even after pollution sources have been eliminated (Briffa et al. 2020; Miletić et al. 2023;

✉ Aybaba Hançerlioğulları  
aliaybaba67@gmail.com; aybaba@kastamonu.edu.tr

<sup>1</sup> Department of Physics, Faculty of Science, Kastamonu University, 37150 Kastamonu, Turkey

<sup>2</sup> Department of Biology, Faculty of Science, Kastamonu University, 37150 Kastamonu, Turkey

<sup>3</sup> Department of Chemistry, Faculty of Science, Kastamonu University, 37150 Kastamonu, Turkey

<sup>4</sup> Department of Geography, Faculty of Humanities and Social Sciences, Kastamonu University, 37150 Kastamonu, Turkey

Torres et al. 2023). Therefore, HM pollution is becoming a significant issue and a source of anxiety caused by the harmful effects it creates worldwide (Briffa et al. 2020; Miletić et al. 2023). Besides their harmful effects on the environment, HMs can accumulate in human organs and cause serious harm to people's health for long exposure to their effects (Huang et al. 2019; Miletić et al. 2023). HMs accumulation in organs brings about diverse chronic and acute diseases affecting the whole system, such as respiratory diseases, immune system damage, nervous system impairment, cardiovascular issues, slowed growth and development, endocrine disruptions, skeletal problems, etc. (Doležalová et al. 2019; Tan et al. 2016; Miletić et al. 2023). The International Agency for Research on Cancer has categorized certain HMs (such as Cu, Co, Zn, Fe, V, and Mn) as non-carcinogenic HMs, while others (such as Hg, Cr, As, Cd, and Pb) are classified as both carcinogenic and non-carcinogenic HMs (Tan et al. 2016). People are directly exposed to HMs in three ways: inhalation, ingestion, and skin (dermal) contact. They may contact with contaminated environmental samples (soil, sediment, dust, rocks, etc.) during recreation, work, or residence. Another way is consuming food grown in indirectly contaminated soil (Miletić et al. 2023).

HMs are released into the air in the form of dust from many anthropogenic and lithogenic origins mentioned above and pollute the air, soil, and water. Air pollution is considered one of the profoundly critical worldwide health problems due to its influence on human health and ecosystems (Suryawanshi et al. 2016; Vaezi et al. 2023). Thus, airborne dust is a significant health and environmental problem that can lead to adverse impacts on living organisms and the environment. So, HMs found in airborne dust create an important hazard to people's health via ingestion, inhalation, and dermal contact (Vaezi et al. 2023). Therefore, determining HM concentrations in outdoor and indoor dust samples is critical for protecting human health and preventing environmental pollution (Xu et al. 2021). Recent studies on HMs existed in dust samples have mainly concentrated on parks, roads, cities, and homes (Suryawanshi et al. 2016; Han et al. 2017; Tang et al. 2017; Jiang et al. 2018; Nimyel and Namadi 2020; Adimalla et al. 2020; Jadoon et al. 2021; Sarmadi et al. 2021; Al-Harbi et al. 2021; Alghamdi et al. 2022; Ceballos et al. 2022; Vaezi et al. 2023; Gul et al. 2023; Andrade et al. 2023). So far, limited studies have been carried out on the analysis of HMs in dust samples related to some industrial activities and the evaluation of workers' health risks associated with HMs (Masto et al. 2017; Ishtiaq et al. 2018; Tong et al. 2019; Sabouhi et al. 2020; Xu et al. 2021; Wang et al. 2023; Sultana et al. 2023). Masto et al. (2017) analyzed the concentrations of HMs (As, Cd, Co, Cr, Cu Ni, Pb, V, and Zn) in dust and soil samples collected from the Jharia coal mining area in India using an inductively coupled plasma-optical emission spectrometry (ICP-OES)

and assessed the exposure risk due to the ingestion, inhalation, and dermal absorption of HMs in the samples. Ishtiaq et al. (2018) investigated the concentrations of HMs (Pb, Cr, Cd, Ni, Cu, Co, and Zn) in coal dust samples collected near various coal mines in Cherat, Pakistan using flame atomic absorption spectrophotometer to evaluate the health risk caused by intake of HMs through inhalation, ingestion, and dermal absorption. Tong et al. (2019) analyzed dust samples from twenty-one types of works in various workplaces in the Shanxi Province of China and assessed the health damages caused by dust inhalation by probabilistic risk assessment method. Sabouhi et al. (2020) determined the levels of HMs (Cd, Cr, Cu, Fe, Mn, Pb, and Zn) in floor dust samples collected from mechanical and battery repairing workshops in Yazd city of Iran by an atomic absorption spectrophotometer to assess the anthropogenic contribution to the presence of HMs, the possible sources and the related risks that could arise from occupational exposure. Xu et al. (2021) measured the concentration of HMs (Cu, Cd, Cr, Pb, Mn, Co, and Zn) in dust samples related to industrial activities in desert steppes by an inductively coupled plasma-mass spectrometer (ICP-MS) to assess HM pollution and carcinogenic health risk. Wang et al. (2023) analyzed the concentrations of HMs (Zn, Pb, Sn, Mn, Cr, Ni, V, As, Cd, and Cu) in workshop dust samples from an industrial area that was home to more than forty printed circuit board manufacturing companies in eastern China using an ICP-MS to assess ecological and health risks. Sultana et al. (2023) determined the levels of HMs (Cd, Zn, Cu, Mn, Pb, Cr, Ni, and Co) in dust samples from coal and chromite mines located in the province of Punjab and Balochistan of Pakistan using a graphite furnace atomic absorption spectrophotometer. However, according to our knowledge, no study has been performed to determine the HM concentrations contained in clay brick (CB) industry dust or kiln dust (KD) samples from CB factories and to evaluate the health risks brought about by these HMs for workers.

CBs are greatly utilized in construction materials globally for their frequent availability, low price, and ease of handling (Riaz et al. 2019). The characterization of CB, whose raw material is clay, is markedly affected by the clay properties, techniques, and coal combustion temperature. Components such as alumina, silica, lime, and iron oxides exist in varying amounts in the clay affecting the quality of the CBs (Riaz et al. 2019). Approximately 340 billion tonnes of clay are mined annually worldwide for brick production (Riaz et al. 2019). KD, a mix of coal ash, brickbats, and burnt clay, is a waste product produced during the CB fabricating process in kilns along coal combustion (Sood et al. 2021). Since the CB industry dust particles contain HMs and silica, they can significantly reduce the air quality in the environment, and these dusts can also cause environmental problems by spreading into the environment around each brick factory,

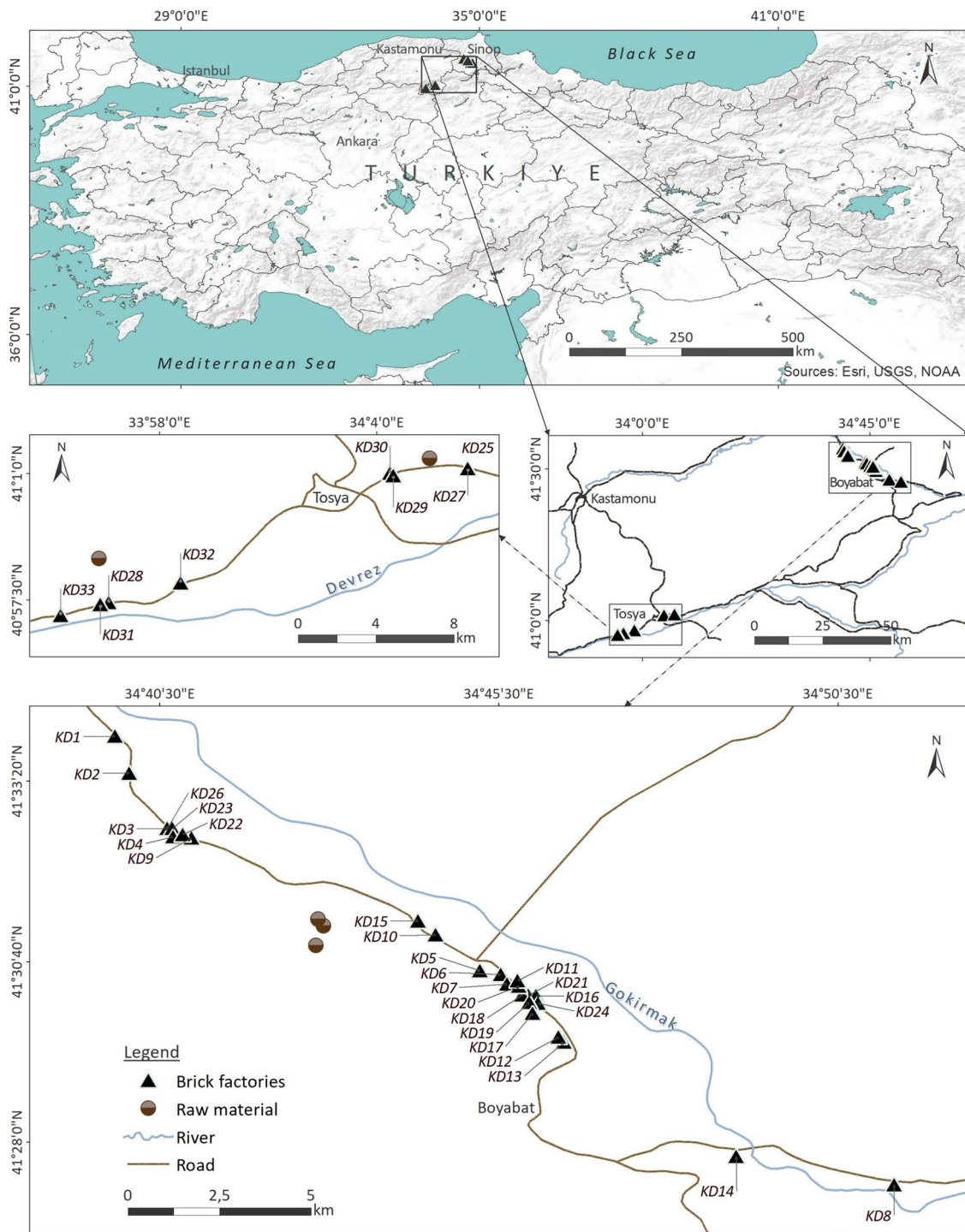


Fig. 1 Map of locations of CB factories

depending on meteorological conditions (Thygerson et al. 2016). Inhalation of dust in the CB industry is a major chemical anxiety among workers because it can irritate the eyes and skin, chronic obstructive pulmonary disease, asthma, bronchitis, silicosis, and other lung complications (Thygerson et al. 2016). Therefore, the assessment of health risk is

a crucial approach to both evaluation of the important hazards posed by toxic contaminants while in contact with the human body and a better understanding of how to approach workplace hazard reduction and control. Considering these, this research is the first detailed research to assess the human health risks caused by dust exposure of workers working in

CB factories. The aims of this study are (i) to analyze the concentrations of major-minor oxides (silicon (SiO<sub>2</sub>), calcium oxide (CaO), alumina (Al<sub>2</sub>O<sub>3</sub>), Iron(III) oxide (Fe<sub>2</sub>O<sub>3</sub>), sulfur trioxide (SO<sub>3</sub>), magnesium oxide (MgO), potassium oxide (K<sub>2</sub>O), sodium oxide (Na<sub>2</sub>O), titanium dioxide (TiO<sub>2</sub>), and phosphorus pentoxide (P<sub>2</sub>O<sub>5</sub>)) and HMs (Fe, Mn, Cr, Ni, V, Zn, Cu, As, Co and Pb) in KD samples, (ii) to compare the concentrations of HMs in KD samples with the Earth's crust average (ECA) given in the study performed by Yaroshvsky (2006), the maximum contaminant level (MCL) recommended in the Turkish Soil Pollution Control Regulation (OG, 2005) and the Turkish industrial soil average (TISA) obtained from the study done by Goren et al. (2022) and (iii) to assess the carcinogenic and non-carcinogenic health risks conceding these HMs via three routs (inhalation, ingestion, and dermal contacts) by estimating health indexes such as hazard index, cancer risk and total cancer risk.

## Materials and Methods

### Collection, Preparation and Analysis of Sample

Thirty-three KD samples were collected from thirty-one coal-fired CB factories shown on the map in Fig. 1. CB factories are located in the Boyabat district of Sinop province and Tosya district of Kastamonu province in the Western Black Sea Region of Türkiye. Samples coded KD1-KD26 were obtained from CB factories in Boyabat and samples coded KD27-KD33 from CB factories in Tosya. The production capacity of these CB factories is equivalent to one-third of the total CB used in the construction industry in Türkiye. Each dust sample was collected by carefully sweeping an area from the production areas of the CB factory with plastic tools (brush and dustpan), and then put into impermeable polyethylene packages for storage. Then, each sample was coded and transported to the Kastamonu University Physics Department Analysis Preparation Laboratory and kept in an atmospheric environment until analysis. Each sample was filtered to remove substances other than dust. The samples were dried in a furnace at 110 °C for 5 h. After being homogenized, approximately five grams of each sample was taken for analysis. CB kiln dust samples were coded as KD. Samples from KD1 to KD25 were collected from Boyabat CB factories, and the others were collected from Tosya CB factories.

Analysis of major-minor oxides and HMs in the KD samples was done by an energy-dispersive X-ray fluorescence (EDXR) spectrometer (Spectro Xepos, Ametek) with a thick binary Pd/Co alloy anode X-ray tube (50 kV, 60 W), the properties of which were detailed in previous studies (Altıkulaç et al. 2022). The system's spectral resolution is less than 155 eV. The spectrometer has software to analyze

samples simultaneously and utilizes "non-standard" calibration techniques based on the basic parameters method. Reference material of NIST SRM 2709 was used for quality assurance of the spectrometry (Turhan et al. 2020). Each KD sample was put in an automatic sampler of the spectrometry, and the analysis was fulfilled by counting for about 1 h. The XRF spectrum of each sample was assessed with the help of software. The overall uncertainty (%) of Na<sub>2</sub>O, MgO, Al<sub>2</sub>O<sub>3</sub>, SiO<sub>2</sub>, P<sub>2</sub>O<sub>5</sub>, SO<sub>3</sub>, K<sub>2</sub>O, CaO, TiO<sub>2</sub>, Fe<sub>2</sub>O<sub>3</sub>, V, Cr, Mn, Fe, Co, Ni, Cu, Zn, As, and Pb was found to be 3.0, 0.4, 0.1, 0.1, 0.5, 0.1, 0.2, 0.1, 0.2, 0.1, 1.9, 0.6, 0.3, 0.1, 11.5, 0.6, 1.4, 0.7, 0.8, and 5.8, respectively.

### Human Health Risk Assessment (HHRA)

USEPA (United States Environmental Protection Agency) recognizes the HHRA as a tool for evaluating the degree and probability of adverse health consequences in individuals exposed to toxic materials in polluted environments (USEPA 2014a, 2014b; Sultana et al. 2023). HHRA consists of two stages. The first stage is the identification and formulation of risks that may cause a threat to people's health (Miletić et al. 2023). Within the scope of this stage, it is required to describe the amount of HMs that cause health results, the frequency of exposure to the contaminated environment media or substance (soil, dust, sediment, etc.), the exposure duration, and the exposure route (or pathway). Three exposure pathways are inhalation, ingestion, and skin contact (Miletić et al. 2023). Ingestion refers to the accidental ingestion of a small amount of contaminated substance. The second stage is risk characterization. HHRA is typically dependent on the estimation of carcinogenic and non-carcinogenic risks for various age groups (generally children and adults).

### Average Daily Dose

As mentioned before, it is first necessary to compute the daily dose of HMs from the substance for three exposure routes to evaluate the carcinogenic and non-carcinogenic risk (Miletić et al. 2023). The USEPA model (1989) was used to calculate the average daily dose (ADD) also referred to as chronic daily intake (CDI) and average daily intake (ADI) in the literature, related to the potential exposure pathways which were inhalation (Inh), incidental ingestion (Ing) and dermal (Derm) absorption or contact. ADD (in terms of mg/kg/d) was calculated for adult CB factory workers using the formulas given below (USEPA 1989; Tan et al. 2016; Sultana et al. 2023; Miletić et al. 2023; Saha et al. 2024):

$$ADD_{Inh} = \frac{C \times InhR \times EF \times ED}{PEF \times BM \times AT} \quad (1)$$

$$ADD_{Ing} = \frac{C \times IngR \times EF \times ED \times 10^{-6}}{BM \times AT} \tag{2}$$

$$ADD_{Derm} = \frac{C \times SA \times AF \times ABS \times EF \times ED \times 10^{-6}}{BM \times AT} \tag{3}$$

where C is the HM concentration in the dust samples (mg/kg); InhR and IngR are the inhalation and ingestion rate of dust given as 20 m<sup>3</sup>/d and 100 mg/d, respectively (USEPA 2011; Miletić et al. 2023); EF is exposure frequency taken as 105 d/y (it was assumed that workers worked 117 days in a year and did not work for an average of 12 days a year on religious and national holidays); ED is exposure duration to dust (24 y) (Miletić et al. 2023); BM is the average body mass of adults (77 kg for Turkish adults) (Turhan et al. 2023) and AT is the exposure time (EF × ED). For non-carcinogenic and carcinogenic AT = EF (105 d/y) × ED (24 y) and AT = EF (365 d/y) × ED (74.8 y; the average life expectancy for Turkish adults), respectively (Miletić et al. 2023; TUIK 2024); PEF is the factor of particle emission (1.36 × 10<sup>9</sup> m<sup>3</sup>/kg) (Miletić et al. 2023); SA is the available surface area of skin for contact (5700 cm<sup>2</sup>) (Miletić et al. 2023); AF is the factor of adherence represented the number of HMs adhered to the skin (0.07 mg/cm<sup>2</sup>/d) (Miletić et al. 2023) and ABS is the factor of dermal absorption (0.01 and 0.001 for carcinogenic and non-carcinogenic, respectively) (Miletić et al. 2023).

### Risk of Non-carcinogenic and Carcinogenic

The non-carcinogenic risk (NCR) estimation refers to determining the effect of HMs in KD on non-carcinogenic consequences in people. Hazard quotient (HQ) and hazard index (HI) are utilized to estimate NCR (Miletić et al. 2023). HQ<sub>i</sub> is the ratio of the ADDs of the HMs given in Eqs. (1)–(3) to their respective reference doses (R<sub>f</sub>D) for all exposure routes as follows (Tan et al. 2016; Sultana et al. 2023; Bushra et al. 2022; Miletić et al. 2023; Saha et al. 2024):

$$HQ_{i,Inh} = \frac{ADD_{i,Inh}}{R_fD_{i,Inh}} \tag{4}$$

$$HQ_{i,Ing} = \frac{ADD_{i,Ing}}{R_fD_{i,Ing}} \tag{5}$$

$$HQ_{i,Derm} = \frac{ADD_{i,Derm}}{R_fD_{i,Derm}} \tag{6}$$

$$HQ_i = HQ_{i,Inh} + HQ_{i,Ing} + HQ_{i,Derm} \tag{7}$$

where R<sub>f</sub>D<sub>Inh</sub>, R<sub>f</sub>D<sub>Ing</sub>, and R<sub>f</sub>D<sub>Derm</sub> are the inhalation and ingestion and dermal reference doses taken as 0.000301, 0.0001, 0.007, 0.00005, 0.0225, 0.70, 0.000014, 0.30, 0.012 and 0.0035 mg/kg/d, 0.0003, 0.003, 0.009, 0.14, 0.02, 0.70, 0.02, 0.30, 0.04 and 0.000035 mg/kg/d and 0.000123, 0.000013, 0.00007, 0.0056, 0.009, 0.42, 0.0008, 0.06, 0.012 and 0.00108 mg/kg/d for As, Cr, V, Mn, Co, Fe, Ni, Zn, Cu and Pb, respectively (USEPA 2004; Bushra et al. 2022; Miletić et al. 2023; Saha et al. 2024). Thereafter, HQ<sub>i</sub> values estimated for each HM in the KD sample are summed to obtain the HI as follows:

$$HI = \sum_{i=1}^n HQ_i \tag{8}$$

where n is the number of HMs. If the HQ > 1 or HI > 1, there is a certain suspicion that HMs may have a detrimental effect on people’s health; If HI < 1, the effect of HMs is unimportant (Miletić et al. 2023).

Carcinogenic health risk measures the carcinogenic effect of HMs in dust on people. Carcinogenic risk (CR) and total carcinogenic risk (TCR) index are used for this aim (Miletić et al. 2023). CR<sub>i</sub> is estimated by multiplying the ADDs given in Eqs. (1)–(3) and the cancer slope factor (CSF) for an HM for three exposure pathways as follows (Miletić et al. 2023):

$$CR_{i,Inh} = ADD_{i,Inh} \times CSF_{i,Inh} \tag{9}$$

$$CR_{i,Ing} = ADD_{i,Ing} \times CSF_{i,Ing} \tag{10}$$

$$CR_{i,Derm} = ADD_{i,Derm} \times CSF_{i,Derm} \tag{11}$$

$$CR_i = CR_{i,Inh} + CR_{i,Ing} + CR_{i,Derm} \tag{12}$$

where CSF<sub>Inh</sub>, CSF<sub>Ing</sub>, and CSF<sub>Derm</sub> are the inhalation and ingestion and dermal cancer slope factors taken as 0.042, 42, 15.1 and 0.84 per mg/kg/d, 0.0085, 0.5, 1.5 and 1.7 per mg/kg/d and 0.0283, 20, 3.66 and 22.5 per mg/kg/d for Pb, Cr, As and Ni, respectively (Bushra et al. 2022; Miletić et al. 2023). CR<sub>i</sub> values estimated for each HM in the KD sample are summed to obtain the TCR characterizing the sum of the CR for each HM across three exposure routes as follows (Miletić et al. 2023):

$$TCR = \sum_{i=1}^n CR_i \tag{13}$$

If TCR < 10<sup>-6</sup>, there is no risk of developing carcinogenic diseases. If 1 × 10<sup>-6</sup> < TCR < 10<sup>-4</sup>, carcinogenic risks are tolerable or acceptable. If TCR exceeds 10<sup>-4</sup>, there is an unacceptable carcinogenic risk (Tan et al. 2016; Miletić et al. 2023).

**Table 1** The concentration and some descriptive statistics data (in mg/kg) of HMs in KD samples

Sample code	Concentration of heavy metal (mg/kg)									
	V	Cr	Mn	Fe	Co	Ni	Cu	Zn	As	Pb
KD1	260	303	712	65340	48	244	58	183	18	18
KD2	766	235	1086	156400	83	971	121	100	339	20
KD3	178	237	549	46300	32	143	33	70	5	12
KD4	235	306	723	60530	39	221	52	111	12	19
KD5	209	276	729	56990	38	183	46	122	13	18
KD6	260	205	802	58470	43	250	59	205	111	16
KD7	206	264	642	55410	39	171	48	115	11	16
KD8	158	188	580	40180	27	123	31	81	12	12
KD9	267	291	661	69950	43	280	68	119	62	18
KD10	204	193	720	47050	36	187	48	87	42	15
KD11	228	251	674	60030	39	205	52	112	36	17
KD12	235	219	736	61320	38	218	61	119	68	21
KD13	194	242	487	47450	30	153	35	74	13	11
KD14	198	242	786	53050	44	199	48	119	36	20
KD15	237	284	725	62540	41	226	51	108	30	17
KD16	321	262	651	74450	40	294	76	243	91	20
KD17	228	273	593	57880	36	202	51	101	13	16
KD18	227	159	466	56250	31	148	40	109	46	12
KD19	204	241	695	61100	40	202	50	104	25	19
KD20	229	257	676	59700	36	230	49	99	49	16
KD21	309	156	684	87940	38	216	89	261	130	27
KD22	155	200	666	38320	26	129	34	81	16	13
KD23	165	197	475	46780	28	115	36	95	20	12
KD24	174	171	639	60550	36	206	53	129	58	13
KD25	197	327	720	59370	50	238	45	98	2	18
KD26	338	220	398	67610	45	319	98	94	62	19
KD27	238	404	1330	76920	66	311	89	139	11	16
KD28	564	255	1191	141000	72	757	117	138	251	17
KD29	174	222	963	52930	32	171	45	119	33	11
KD30	221	378	1377	78180	54	253	82	120	12	17
KD31	225	300	1150	79650	50	270	94	178	31	18
KD32	208	375	1281	75250	52	242	82	120	14	18
KD33	163	163	773	44750	35	154	46	90	54	9
Average	248	251	768	65444	42	249	60	122	52	16
Median	225	242	712	60030	39	216	51	112	31	17
SD	119	62	252	24514	13	169	24	45	70	4
SE	21	11	44	4267	2	29	4	8	12	1
Kurtosis	3.3	0.6	1.1	2.5	1.6	3.4	1.1	1.8	3.0	0.3
Skewness	12.2	0.3	0.6	7.5	3.2	12.3	0.5	3.2	9.6	1.1
Min	155	156	398	38320	26	115	31	70	2	9
Max	766	404	1377	156400	83	971	121	261	339	27

### Positive Matrix Factorization (PMF) Model

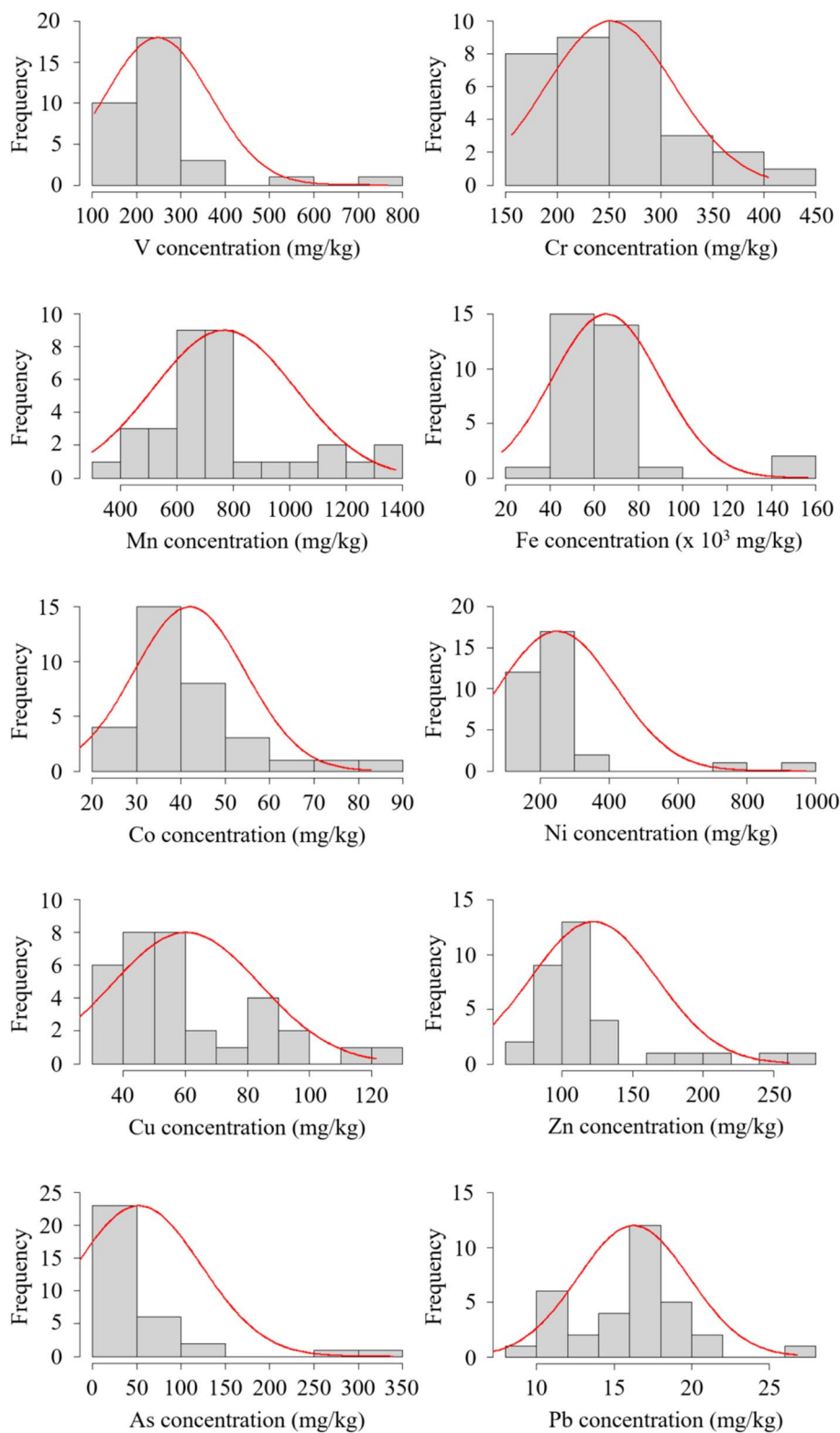
In the study, the PMF receptor model was developed by using EPA PMF software (version 5.0) (USEPA 2014a, 2014b) to identify sources of HMs in KD samples, as previously described by Jiang et al. (2023). The optimal solution was obtained by examining 3 to 6 factors using 20 base runs

conducted in random seed mode (Zhang et al. 2018; Cheng et al. 2020; Jiang et al. 2023).

### Spatial Distribution Analysis

Spatial distribution analysis of HM concentrations of dust samples was performed using QGIS Desktop 3.36.0

**Fig. 2** The frequency distribution of the concentration of HMs



software. In spatial distribution analysis, the geographical coordinates of each dust collection point, CB factories, were plotted on a digital map. Subsequently, inverse distance weighting (IDW) interpolation was used to estimate

the concentrations of HMs in the study area based on the values obtained from sampled points.

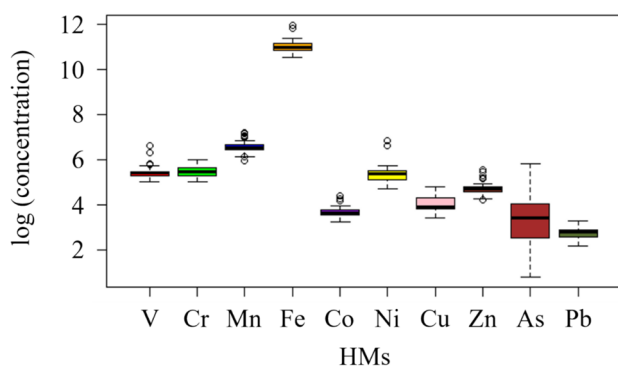


**Fig. 3** The box plot for the logarithmic transformed data

## Statistical Analysis

The statistical analysis was done to assess data distribution, investigate variance homogeneity, and determine potential differences among groups concerning the concentrations of HMs. The data were subjected to the Shapiro–Wilk test to discern normality and the Bartlett test to observe variance homogeneity. The Shapiro–Wilk and Bartlett tests showed that most of the data did not conform to the normal distribution or exhibit homogeneity of variances. Therefore, the data was transformed using logarithmic conversion. However, the logarithmic transformed data still did not conform to the normal distribution or exhibit homogeneity of variances.

Thus, the Kruskal–Wallis test ( $p=0.05$ ) was used to investigate the potential differences among HM concentrations, and pairwise Wilcoxon rank-sum tests were applied to display significant differences.

In addition, Pearson correlation coefficients were calculated to put forward any correlation between the HMs in terms of their concentration in the dust samples. All statistical analyses were conducted by R studio version 2023.06 (R Core Team 2023).

## Results and Discussion

### Concentration of Major–Minor Oxides and Heavy Metal

According to the average concentration (in % dry weigh, dw) of the major ( $>1\%$ ) and minor ( $>0.1\%$ ) oxides in the KD samples were ranked as  $\text{SiO}_2$  (41.7)  $>$   $\text{Al}_2\text{O}_3$  (15.9)  $>$   $\text{CaO}$  (10.7)  $>$   $\text{Fe}_2\text{O}_3$  (9.3)  $>$   $\text{MgO}$  (6.5)  $>$   $\text{SO}_3$  (4.8)  $>$   $\text{Na}_2\text{O}$  (1.8)  $>$   $\text{K}_2\text{O}$  (1.8)  $>$   $\text{TiO}_2$  (0.9)  $>$   $\text{P}_2\text{O}_5$  (0.2). The concentrations (% dw) of  $\text{SiO}_2$ ,  $\text{Al}_2\text{O}_3$ ,  $\text{CaO}$ ,  $\text{Fe}_2\text{O}_3$ ,  $\text{MgO}$ ,  $\text{SO}_3$ ,  $\text{Na}_2\text{O}$ ,  $\text{K}_2\text{O}$ ,  $\text{TiO}_2$  and  $\text{P}_2\text{O}_5$  varied from 18.8 (KD6) to 51.1 (KD23), 7.5 (KD6) to 24.5 (KD18), 6.5 (KD23) to 15.2 (KD10), 5.5 (KD22) to 22.4 (KD2), 2.1 (KD2) to

12.3 (KD28), 0.2 (KD29) to 15.9 (KD2), 0.2 (KD27) to 3.8 (KD28), 1.3 (KD30) to 2.8 (KD21), 0.5 (KD6) to 1.6 (KD29) and 0.1 (KD25) to 0.3 (KD27), respectively. The average concentration of  $\text{CaO}$ ,  $\text{Fe}_2\text{O}_3$ ,  $\text{MgO}$ ,  $\text{SO}_3$  and  $\text{K}_2\text{O}$  are higher than the ECAs of 9.4%, 1.1%, 5.4%, 0.05% and 1.1%, respectively (Yaroshevsky 2006). The average concentrations of  $\text{Al}_2\text{O}_3$ ,  $\text{TiO}_2$  and  $\text{P}_2\text{O}_5$  are near to the ECAs of 15.9%, 0.97% and 0.19% %, while the average concentrations of  $\text{SiO}_2$  and  $\text{Na}_2\text{O}$  are lower than the ECAs of 53.5% and 2.7%, respectively (Yaroshevsky 2006).

The concentration and some descriptive statistical data of HMs analyzed in KD samples are presented in Table 1. The frequency distribution of the concentration of HMs is shown in Fig. 2. According to the statistical analysis, only Mn and Pb exhibit a normal distribution, while other HMs failed to present a normal distribution, as seen in Fig. 2. From Table 1, the average concentration hierarchy of HMs in KD samples is  $\text{Fe} > \text{Mn} > \text{Cr} > \text{Ni} > \text{V} > \text{Zn} > \text{Cu} > \text{As} > \text{Co} > \text{Pb}$ . The box plot for the concentration distribution of HMs for logarithmically transformed data is given in Fig. 3. Figure 3 shows the highest log concentration of HMs was observed for Fe, whereas the lowest was for Pb. Furthermore, differences between all HM concentrations were detected. To assess the statistical significance of these differences, the Kruskal–Wallis test was applied, revealing statistically significant differences between the log concentrations of HMs ( $p < 0.05$ ). The Kruskal–Wallis test results revealed statistically significant differences in the concentrations of HMs among the dust samples. Additionally, the Wilcoxon rank-sum test confirmed that nearly all pairs of HM concentrations significantly differed.

The Fe concentrations in the KD samples varied from 38320 (KD22) to 156400 (KD2) mg/kg with an average value of 65444 mg/kg. All Fe concentrations, except for four KD samples, are higher than the ECA (46500 mg/kg), while Fe concentrations are above the TISA (355579 mg/kg). The Mn concentrations varied from 398 (KD26) to 1377 (KD30) mg/kg, with an average value of 768 mg/kg. All Mn concentrations, except for six KD samples, are lower than the ECA (1000 mg/kg) and TISA (992 mg/kg). The Cr concentrations varied from 156 (KD21) to 404 (KD27) mg/kg with an average value of 251 mg/kg. All Cr concentrations are higher than the ECA (83 mg/kg) and maximum contaminant level (MCL) (100 mg/kg) (OG, 2005), while all Cr concentrations, except for three KD samples, are lower than the TISA (333 mg/kg). The Ni concentrations varied from 115 (KD23) to 971 (KF2) mg/kg, with an average value of 249 mg/kg. All Ni concentrations are higher than MCL (30 mg/kg) and ECA (58 mg/kg), while all Ni concentrations, except for two KD samples, are lower than TISA (125 mg/kg). The V concentrations varied from 155 (KD22) to 766 (KD2) mg/kg, with an average value of 248 mg/kg. All V concentrations are higher than the ECA



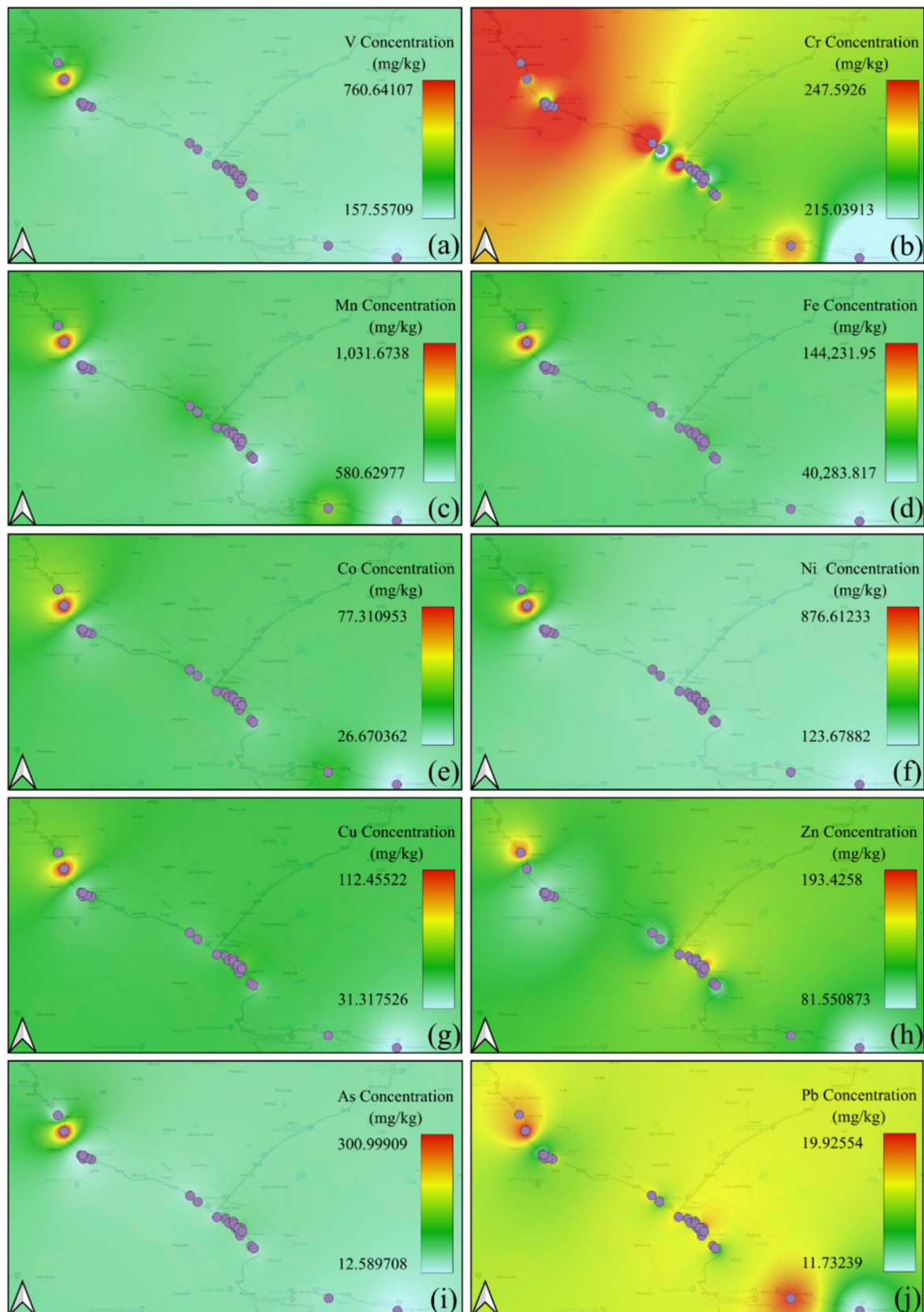


**Fig. 4** The distribution (in mg/kg) of HMs in CB factories from Boyabat, Turkey. HM distributions are presented for **a** V, **b** Cr, **c** Mn, **d** Fe, **e** Co, **f** Ni, **g** Cu, **h** Zn, **i** As, and **j** Pb

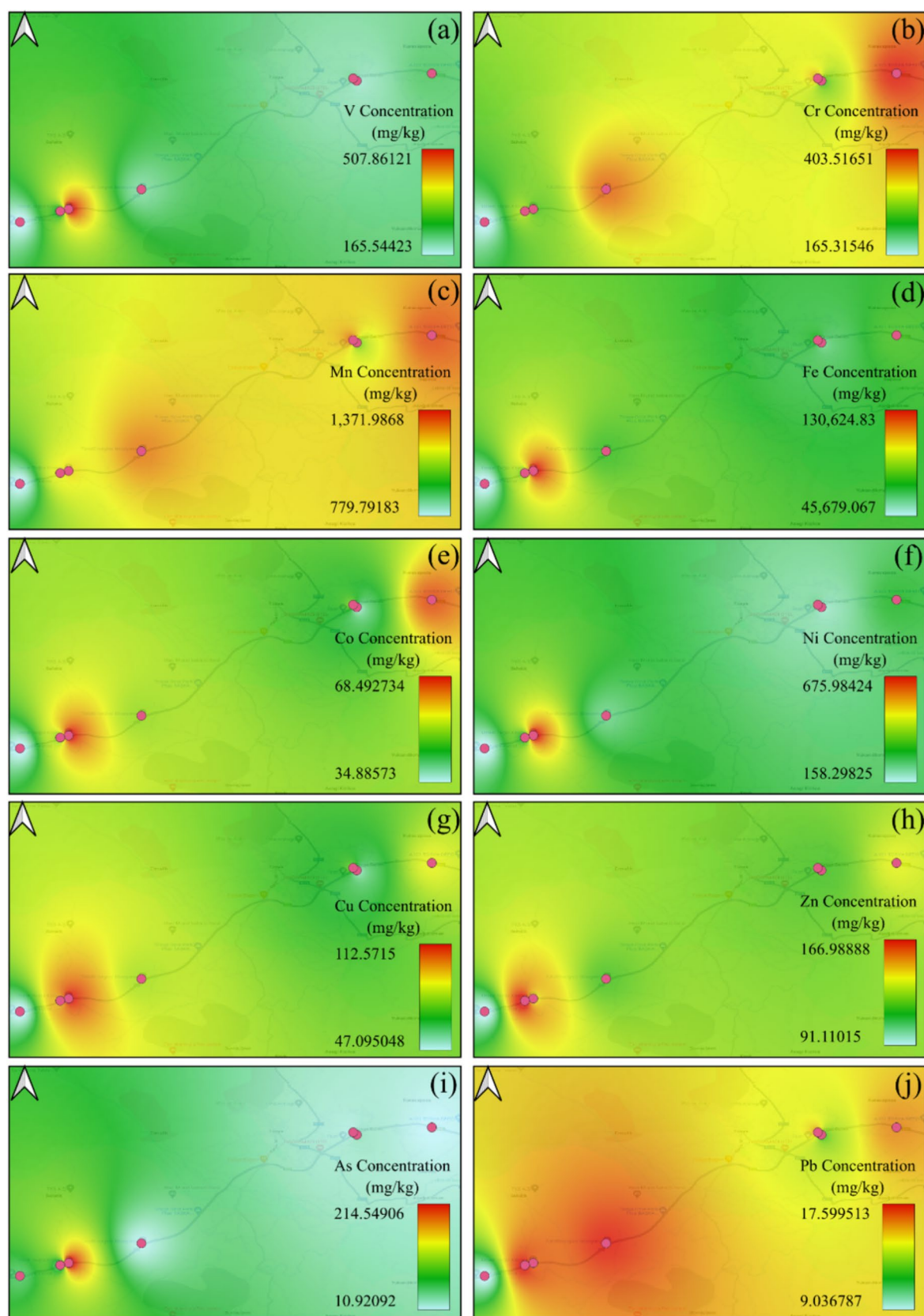


**Fig. 5** The distribution (in mg/kg) of HMs in CB factories from Tosya, Turkey. HM distributions are presented for **a** V, **b** Cr, **c** Mn, **d** Fe, **e** Co, **f** Ni, **g** Cu, **h** Zn, **i** As, and **j** Pb

**Table 2** Impact of heavy metals in KD under different exposure routes on human health risks

Heavy metal	ADD (mg/kg/d)			Non-carcinogenic risk			Carcinogenic risk		
	Ingestion	Inhalation	Dermal	Ingestion	Inhalation	Dermal	Ingestion	Inhalation	Dermal
	HQ <sub>i</sub>			CR <sub>i</sub>					
V	$3.22 \times 10^{-4}$	$4.73 \times 10^{-8}$	$1.28 \times 10^{-6}$	$3.57 \times 10^{-2}$	$6.76 \times 10^{-6}$	$1.83 \times 10^{-2}$	-	-	-
Mn	$9.97 \times 10^{-4}$	$1.47 \times 10^{-7}$	$3.98 \times 10^{-6}$	$7.12 \times 10^{-3}$	$2.93 \times 10^{-3}$	$7.01 \times 10^{-4}$	-	-	-
Fe	$8.50 \times 10^{-2}$	$1.25 \times 10^{-5}$	$3.39 \times 10^{-4}$	$1.21 \times 10^{-1}$	$1.79 \times 10^{-5}$	$8.07 \times 10^{-4}$	-	-	-
Co	$5.45 \times 10^{-5}$	$8.01 \times 10^{-9}$	$2.17 \times 10^{-7}$	$2.72 \times 10^{-3}$	$3.56 \times 10^{-7}$	$2.42 \times 10^{-5}$	-	-	-
Cu	$7.81 \times 10^{-5}$	$1.15 \times 10^{-8}$	$3.12 \times 10^{-7}$	$1.95 \times 10^{-3}$	$9.58 \times 10^{-7}$	$2.60 \times 10^{-5}$	-	-	-
Zn	$1.59 \times 10^{-4}$	$2.34 \times 10^{-8}$	$6.34 \times 10^{-7}$	$5.30 \times 10^{-4}$	$7.79 \times 10^{-8}$	$1.06 \times 10^{-5}$	-	-	-
Cr	$3.01 \times 10^{-5}$	$4.43 \times 10^{-9}$	$1.20 \times 10^{-6}$	$1.00 \times 10^{-2}$	$4.43 \times 10^{-5}$	$9.25 \times 10^{-2}$	$1.51 \times 10^{-5}$	$1.86 \times 10^{-7}$	$2.40 \times 10^{-5}$
Ni	$2.99 \times 10^{-5}$	$4.40 \times 10^{-9}$	$1.19 \times 10^{-6}$	$1.49 \times 10^{-3}$	$3.14 \times 10^{-4}$	$1.49 \times 10^{-3}$	$5.08 \times 10^{-5}$	$3.69 \times 10^{-9}$	$2.71 \times 10^{-5}$
As	$6.26 \times 10^{-6}$	$9.21 \times 10^{-10}$	$7.50 \times 10^{-7}$	$2.09 \times 10^{-2}$	$3.06 \times 10^{-6}$	$6.10 \times 10^{-3}$	$9.39 \times 10^{-6}$	$1.39 \times 10^{-8}$	$2.74 \times 10^{-6}$
Pb	$1.95 \times 10^{-6}$	$2.86 \times 10^{-10}$	$7.77 \times 10^{-8}$	$5.56 \times 10^{-2}$	$8.18 \times 10^{-8}$	$7.20 \times 10^{-5}$	$1.66 \times 10^{-8}$	$1.20 \times 10^{-11}$	$2.20 \times 10^{-9}$
				$HQ_i = \sum HQ_i$			$TCR_i = \sum CR_i$		
				$HI = \sum HI_i$			$TCR = \sum TCR_i$		

(90 mg/kg). The Zn concentrations varied from 70 (KD3) to 261 (KD21) mg/kg, with an average value of 122 mg/kg. All Zn concentrations, except four KD samples, are higher than the ECA (83 mg/kg), while except for five KD samples, all Zn concentrations are lower than the MCL (150 mg/kg), and except for one KD sample, TISA (248 mg/kg). The Cu concentrations varied from 31 (KD8) to 121 (KD2) mg/kg with an average value of 60 mg/kg. Approximately one-third of the Cu concentrations are lower than the ECA (47 mg/kg and MCL (50 mg/kg), while all Cu concentrations are lower than TISA (588 mg/kg). The As concentrations varied from 2 (KD25) to 339 (KD2) mg/kg with an average value of 52 mg/kg. Approximately two-thirds of the As concentrations are higher than the MCL (20 mg/kg). All As concentrations are lower than TISA (500 mg/kg) while higher than the ECA (1.7 mg/kg). The Co concentrations varied from 26 (KD22) to 83 (KD2) mg/kg with an average value of 42 mg/kg. All Co concentrations are higher than the ECA (18 mg/kg), MCL (20 mg/kg), and TISA (21 mg/kg). The Pb concentrations varied from 9 (KD33) to 27 (KD21) mg/kg, with an average value of 16 mg/kg. All Pb concentrations are lower than the MCL (50 mg/kg) and TISA (125 mg/kg), while approximately one-third of the Pb concentrations are lower than the ECA (16 mg/kg).

The spatial distribution analysis of HMs for the dust samples collected from CB factories was conducted to present the variation in HM concentrations throughout collection points and concentration patterns across the study area. The distributions of HMs in CB factories from Boyabat and Tosya district are given in Figs. 4 and 5, respectively.

### Exposure Assessment

Table 2 presents non-carcinogenic and carcinogenic health risk results assessed for adult workers. The average values of the  $ADD_{Ing}$ ,  $ADD_{Inh}$  and  $ADD_{Derm}$  calculated for all HMs in the KD samples were found as  $8.7 \times 10^{-3}$  mg/kg/d,  $1.3 \times 10^{-6}$  mg/kg/d, and  $3.5 \times 10^{-5}$  mg/kg/d, respectively. The average  $ADD_{Ing}$  and  $ADD_{Inh}$  values of the HMs are ranked as  $Fe > Mn > V > Zn > Cu > Co > Cr > Ni > As > Pb$ , while the average  $ADD_{Derm}$  values are ranked  $Fe > Mn > V > Cr > Ni > As > Zn > Cu > Co > Pb$ . The highest and lowest  $ADD_i$  values were  $8.5 \times 10^{-2}$  mg/kg d for ingestion of Fe and  $2.7 \times 10^{-10}$  mg/kg/d for inhalation of Pb, respectively. With respect to average  $ADD_i$ , the three exposure routes were listed as ingestion > dermal contact > inhalation.

The average values of the  $HQ_{Ing}$ ,  $HQ_{Inh}$ , and  $HQ_{Derm}$  estimated for all HMs in the KD samples were  $2.6 \times 10^{-2}$ ,  $3.3 \times 10^{-4}$  and  $1.2 \times 10^{-2}$ , respectively. The average  $HQ_{Ing}$ ,  $HQ_{Inh}$ , and  $HQ_{Derm}$  values of the HMs are ranked  $Fe > Pb > V > As > Cr > Mn > Co > Cu > Ni > Zn; Mn > Ni > Cr >$

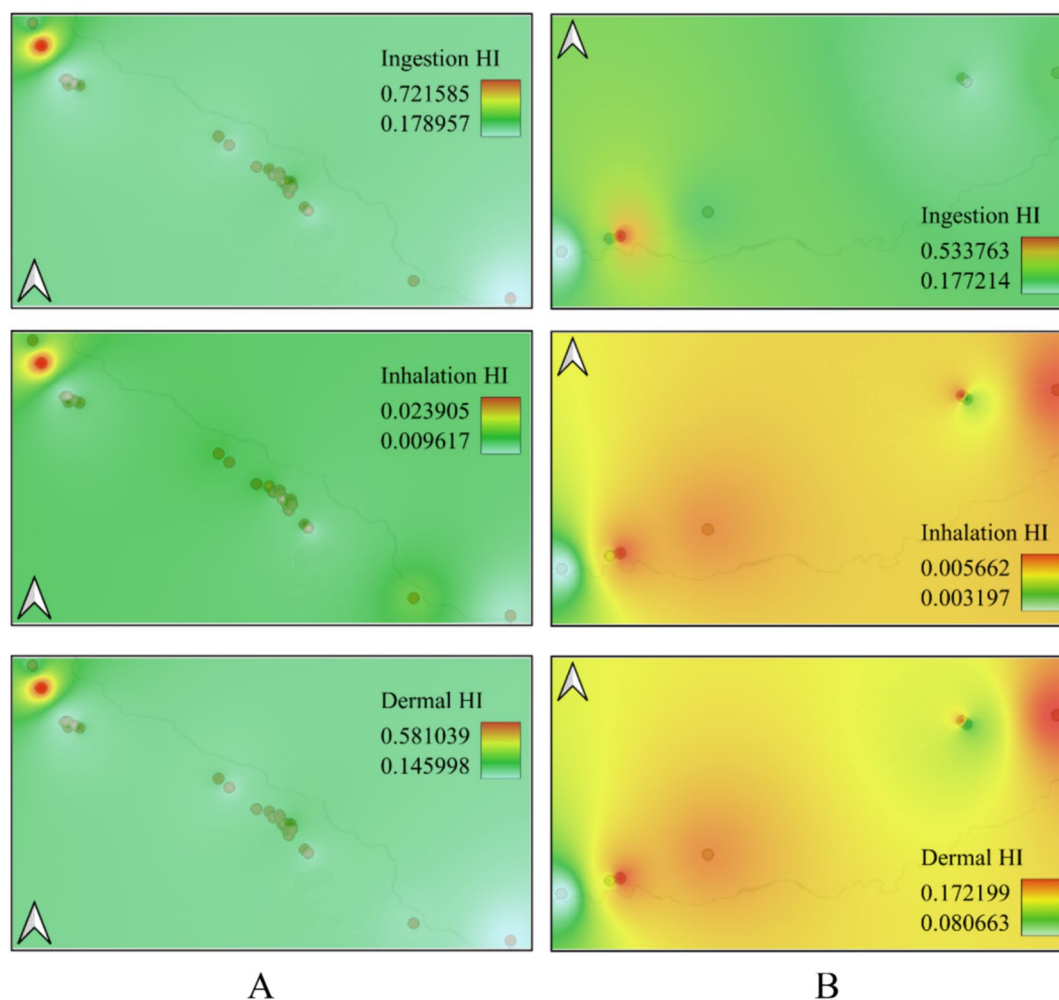


**Fig. 6** The spatial distribution for non-carcinogenic risks: **A** Boyabat, **B** Tosya

Fe > V > As > Cu > Co > Pb > Zn, and Cr > V > As > Ni > Fe > Mn > Pb > Cu > Co > Zn. The highest and lowest  $HQ_i$  values were  $1.3 \times 10^{-1}$  for ingestion of Fe and  $8.6 \times 10^{-8}$  for inhalation of Zn, respectively. With respect to average  $HQ_i$ , the three exposure routes were in the following order: ingestion > dermal contact > inhalation. All  $HQ$  values are lower than the risk limit of 1. The average values of the  $HI_{Ing}$ ,  $HI_{Inh}$  and  $HI_{Derm}$  estimated for all HMs in the KD samples were  $2.6 \times 10^{-1}$ ,  $3.3 \times 10^{-3}$ , and  $1.2 \times 10^{-1}$ , respectively. With

respect to average  $HI_i$ , the three exposure routes were in the following order: ingestion > dermal contact > inhalation. The estimated  $HI$  value for all HMs and three exposure routes is 0.38, which is below the risk limit of 1.

The average values of the  $CR_{Ing}$ ,  $CR_{Inh}$ , and  $CR_{Derm}$  estimated for Pb, Cr, As and Ni were  $1.9 \times 10^{-5}$ ,  $5.1 \times 10^{-8}$  and  $1.4 \times 10^{-5}$ , respectively. The average  $CR_{Ing}$  and  $CR_{Derm}$  values of these HMs are ranked Ni > Cr > As > Pb, while the average  $CR_{Inh}$  values are ranked Cr > As > Ni > Pb. The highest and lowest  $CR_i$  values were  $5.8 \times 10^{-5}$  for ingestion of Ni and  $1.2 \times 10^{-11}$  for inhalation of Pb, respectively. The total average values of the  $CR_{i,Ing}$ ,  $CR_{i,Inh}$ , and  $CR_{i,Derm}$  were  $7.5 \times 10^{-5}$ ,  $2.0 \times 10^{-7}$  and  $5.4 \times 10^{-5}$ , respectively. With respect to average  $CR_i$ , the three exposure routes were in the following order: dermal contact > ingestion > inhalation. All  $CR$  values are in the safe range. The  $TCR$  value estimated for these four HMs and three exposure routes is  $1.3 \times 10^{-4}$ , which is above the carcinogenic risk limit of  $1.0 \times 10^{-4}$ .

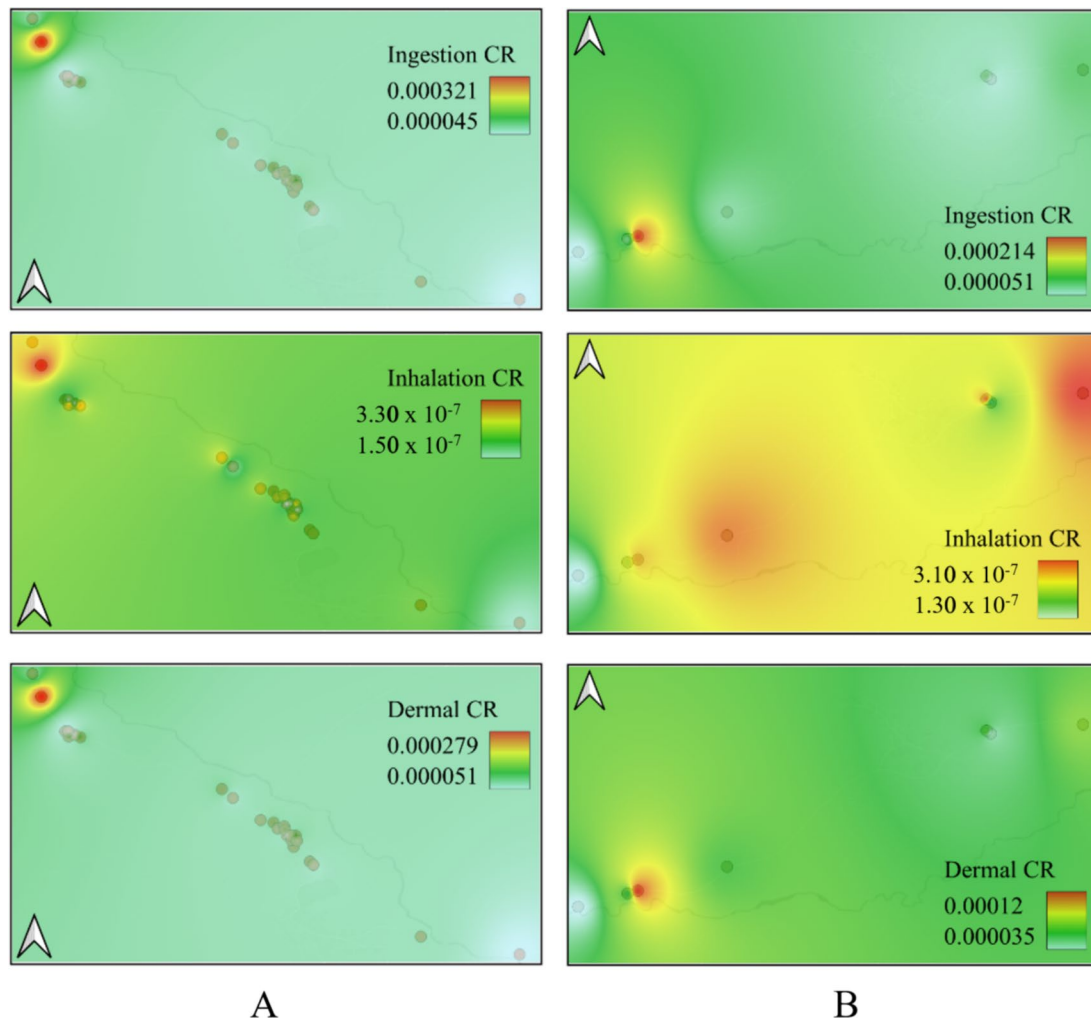


**Fig. 7** The spatial distribution for carcinogenic risks: **A** Boyabat, **B** Tosya

The spatial distribution analysis was also conducted for non-carcinogenic and carcinogenic risks across the study area. The non-carcinogenic and carcinogenic risk distributions for Boyabat and Tosya are shown in Figs. 6 and 7. The spatial distribution maps indicate that workers, particularly those working in KD2 (Boyabat) and KD28 (Tosya), are at risk of health issues.

To explore potential sources of HMs in dust samples, Pearson correlation analysis (Fig. 8) was used to present pairwise correlations among HMs in dust samples, and the PMF model was used to reveal any potential common sources for the presence of HMs in the samples (Jiang et al. 2023). According to the analysis, three factors were found to be the sources of HMs.

The results showed that Factor 1 contributed 40.50%, Factor 2 44.30%, and Factor 3 15.20% in the results of the PMF model (Fig. 8a). Figure 8b presents the contribution of each HM to the factors identified in the PMF model. According to the results, Pb and V exhibit the highest contributions

to Factor 1. According to previous studies, the source of V may be natural sources and soil sampling (Hernandez and Rodriguez 2012). Bird (2011) proposed that the sources of Pb in the environment can be linked to industrial anthropogenic activity and coal combustion. Thus, Factor 1 predominantly represents contributions from natural sources, soil, and coal combustion. During the dust sampling process, it was observed that each CB factory had a different base soil, often containing residues of ash and coal. Thus, it is possible to propose that Factor 1 could represent the factory base soil.

Analysis of Factor 2 reveals that As, Ni and V are the primary contributors. Chung et al. (2014) proposed that As found in the environment is predominantly based on natural sources, namely the Earth's crust. The source of Ni (Kierczak et al. 2021) and V (Hernandez and Rodriguez 2012) is also suggested to be natural sources. Therefore, it is reasonable to associate Factor 2 with the clay used in brick production.

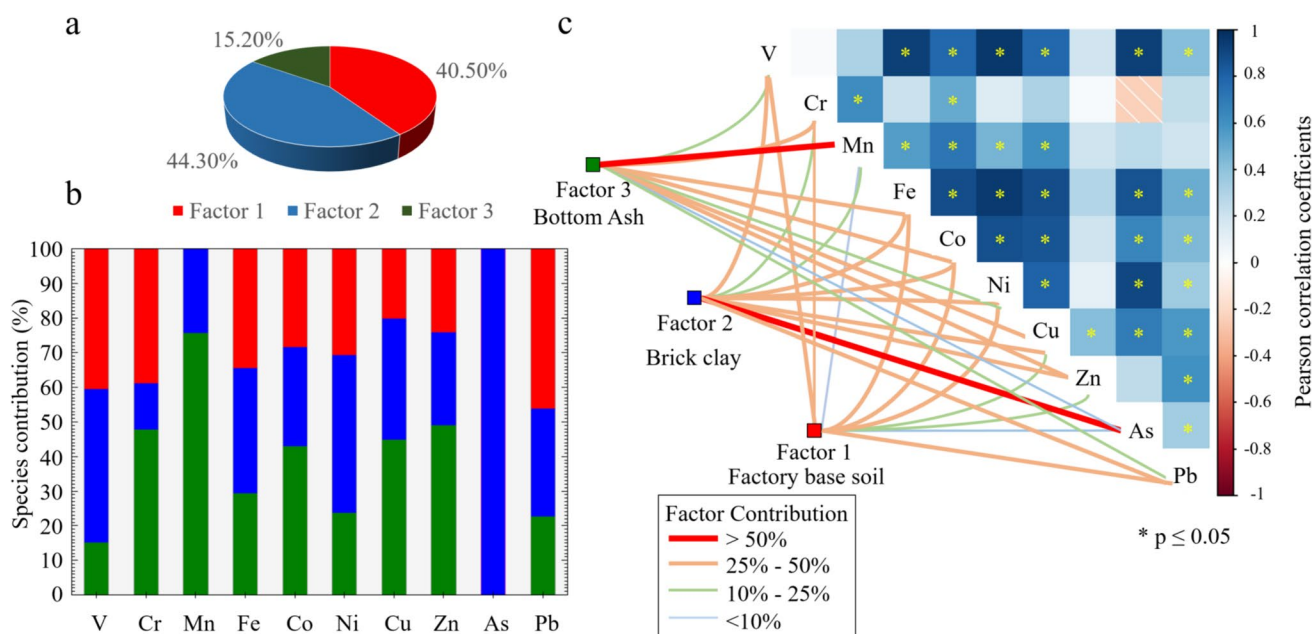


**Fig. 8** Source assignments for HMs. **a** Factor contributions (%) to the PMF model, **b** HM contributions (%) to each factor, **c** The Pearson correlation coefficients for HM pairs and their relation of each HM to the factors of the PMF model

The results showed that Mn, Zn, and Cu contributed to Factor 3. Previous studies have shown that Mn can originate from the combustion of fossil fuels (Howe et al. 2004). Haque et al. (1982) proposed that the sources of Zn in the environment can be linked to coal combustion, oil combustion, wood combustion, and industrial applications. The source of Cu is also suggested to be oil combustion and wood smoke (Al-Masri et al. 2006). Thus, it is possible to propose that Factor 3 predominantly represents contributions from coal combustion used in brick production. Figure 8c presents both the percentages of HMs contributing to each factor and the correlation test results. According to Fig. 8c, it can be proposed that Mn contributes highly to Factor 3, whereas As contributes highly to Factor 2. In addition, the upper part of Fig. 8c shows that there are very strong correlations between V and Fe; V and Ni; Fe and Ni; and V and As. Furthermore, the correlations between V and Co; V and Cu; Fe and Co; Fe and Cu; Fe and As; Co and Ni; Co and Cu; Ni and Cu; and Ni and As are also high.

## Conclusion

In this first and detailed study, the concentrations of major-minor oxides and ten heavy metals (V, Cr, Mn, Fe, Co, Ni, Cu, Zn, As, and Pb) in kiln dust samples from clay brick factories in the Western Black Sea Region of Türkiye were analyzed and carcinogenic and non-carcinogenic human health risks from three exposure routes of heavy metals from kiln dust samples were assessed for adult workers.

Concentrations of heavy metals varied depending on parameters such as the structure of the clay used as raw material, brick firing temperature, and the type and structure of coal. Analysis results revealed that (i) 50% of the kiln dust samples were composed of silicone and (ii) all of the Cr, Ni, and Co concentrations and two-thirds of the Cu and As concentrations were greater than the maximum contaminant levels recommended in the Turkish Soil Pollution Control Regulation.

Assessment of human health risk is a critical approach to estimating the remarkable risks due to the toxic heavy metal contaminants when in contact with the human body. The findings may help improve worker safety measures. In this study, human health risk assessment was performed using the deterministic model recommended by USEPA. Risk assessment results revealed that HQ and HI values were all within safe levels, reflecting that heavy metals do not cause a non-carcinogenic risk to workers' health. However, the TCR value estimated for Cr, Ni, As, and Pb showed that workers can be faced carcinogenic health risks.

In conclusion, this study denotes that (i) the formation of dust contaminated with heavy metals is a severe problem in working areas in brick factories and should be constantly monitored, and (ii) it is vital to comply with safety standards in brick factories to ensure safety and keep inhalable kiln dust at safe levels for workers. Therefore, contemporary and effective technologies should be used to minimize health risks associated with occupational exposure, and the usage of personal protective equipment

should be made mandatory among workers to restrict heavy metal exposure.

**Acknowledgements** The authors would like to thank the brick factory managers in the Western Black Sea region for their convenience and close attention to sample collection.

**Author Contributions** Şeref Turhan led the research project on the assessment of clay brick kiln dust samples. Şeref Turhan, Celalettin Duran, Temel K. Bakır, Ayababa Hançerlioğulları, and Aslı Kurnaz collected the samples and made them ready for analysis. Şeref Turhan and Ergin M. Altuner performed the statistical analyses. Şeref Turhan evaluated the data and wrote the manuscript. All authors read and finalized the manuscript.

**Funding** Open access funding provided by the Scientific and Technological Research Council of Türkiye (TÜBİTAK). However, the TCR value estimated for Cr, Ni, As, and Pb showed that workers can be faced carcinogenic health risks.

**Data Availability** Data will be made available on request.

## Declarations

**Competing Interests** The authors declare that they have no known competing financial interests or personal relationships that could have appeared to influence the study reported in this manuscript.

**Open Access** This article is licensed under a Creative Commons Attribution 4.0 International License, which permits use, sharing, adaptation, distribution and reproduction in any medium or format, as long as you give appropriate credit to the original author(s) and the source, provide a link to the Creative Commons licence, and indicate if changes were made. The images or other third party material in this article are included in the article's Creative Commons licence, unless indicated otherwise in a credit line to the material. If material is not included in the article's Creative Commons licence and your intended use is not permitted by statutory regulation or exceeds the permitted use, you will need to obtain permission directly from the copyright holder. To view a copy of this licence, visit <http://creativecommons.org/licenses/by/4.0/>.

## References

- Adimalla N, Chen J, Qian H (2020) Spatial characteristics of heavy metal contamination and potential human health risk assessment of urban soils: a case study from an urban region of South India. *Ecotoxicol Environ Saf* 194:1–8
- Alghamdi AG, EL-Saeid MH, Alzahrani AJ, Ibrahim HM (2022) Heavy metal pollution and associated health risk assessment of urban dust in Riyadh Saudi Arabia. *PLoS ONE* 17(1):1–15
- Al-Harbi M, Alhajri I, Whalen JK (2021) Characteristics and health risk assessment of heavy metal contamination from dust collected on household HVAC air filters. *Chemosphere* 277:1–9
- Al-Masri MS, Al-Kharfan K, Al-Shamali K (2006) Speciation of Pb, Cu and Zn determined by sequential extraction for identification of air pollution sources in Syria. *Atmospheric Environ* 40(4):753–761
- Altıkulaç A, Turhan Ş, Kurnaz A, Gören E, Duran C, Hançerlioğulları A, Uğur FA (2022) Assessment of the enrichment of heavy metals in coal and its combustion residues. *ACS Omega* 7(24):21239–21245
- Andrade A, Aguilera A, Gallegos Á, Aguilar Y, Quintana P, Bautist F (2023) Heavy metals in urban dust inside and outside homes during the Covid-19 pandemic in Mérida, Yucatán, México. *Air Qual Atmos Health* 16:2337–2349
- Bird G (2011) Provenancing anthropogenic Pb within the fluvial environment: developments and challenges in the use of Pb isotopes. *Environ Int* 37(4):802–819
- Briffa J, Sinagra E, Blundell R (2020) Heavy metal pollution in the environment and their toxicological effects on humans. *Heliyon* 6(9):1–26
- Bushra A, Zakir HM, Sharmin S, Quadir QF, Rashid MH, Rahman MS, Mallick S (2022) Human health implications of trace metal contamination in topsoils and brinjal fruits harvested from a famous brinjal-producing area in Bangladesh. *Sci Rep* 12:1–26
- Ceballos DM, Dong Z, Peters JL, Herrick RF, Gupta P, Spengler JD (2022) Metals dust in workers' homes and potential for take home in the Greater Boston area: pilot study. *Environ Res* 209:1–12
- Cheng W, Lei S, Bian Z, Zhao Y, Li Y, Gan Y (2020) Geographic distribution of heavy metals and identification of their sources in soils near large, open-pit coal mines using Positive Matrix Factorization. *J Hazard Mater* 387:1–14
- Chung JY, Seung-Do Y, Hong YS (2014) Environmental source of arsenic exposure. *J Prev Med Public Health* 47:253–257
- Doležalová WH, Mihočová S, Chovanec P, Pavlovský J (2019) Potential ecological risk and human health risk assessment of heavy metal pollution in industrial affected soils by coal mining and metallurgy in Ostrava, Czech Republic. *Int J Environ Res Public Health* 16(22):1–29
- Goren AY, Genisoglu M, Kazancı Y, Sofuoğlu SC (2022) Country-wide spatial variation of potentially toxic element contamination in soils of Turkey and assessment of population health risks for nondietary ingestion. *ACS Omega* 7(41):36457–36467
- Gul HK, Gullu G, Babaei P, Nikravan A, Kurt-Karakus PB, Salihoglu G (2023) Assessment of house dust trace elements and human exposure in Ankara. *Turkey Environ Sci Pollut Res Int* 30(3):7718–7735
- Han X, Lu X, Qinggeletu WuY (2017) Health risks and contamination levels of heavy metals in dusts from parks and squares of an industrial city in semi-arid area of China. *Int J Environ Res Public Health* 14(8):1–12
- Haque MA, Subramanian V, Gibbs RJ (1982) Copper, lead, and zinc pollution of soil environment. *Crit Rev Env Sci Tec* 12(1):13–68
- Hernandez H, Rodriguez R (2012) Geochemical evidence for the origin of vanadium in an urban environment. *Environ Monit Assess* 184:5327–5342
- Howe P, Malcolm H, Dobson S (2004) World Health Organization & International Programme on Chemical Safety. Manganese and its compounds: environmental aspects. World Health Organization. <https://iris.who.int/handle/10665/42992>
- Huang S, Shao G, Wang L, Wang L, Tang L (2019) Distribution and health risk assessment of trace metals in soils in the golden triangle of southern Fujian province, China. *Int J Environ Res Public Health* 16(97):1–17
- Ishtiaq M, Jehan N, Khan SA, Muhammad S, Saddique U, Iftikhar B (2018) Potential harmful elements in coal dust and human health risk assessment near the mining areas in Cherat, Pakistan. *Environ Sci Pollut Res* 25:14666–14673
- Jadoon W, Mohamed S, Abdel-Dayem M, Saqib Z, Takeda K, Sakugawa H, Hussain M, Mujtaba G, Rehman W, Hussain J (2021) Heavy metals in urban dusts from Alexandria and Kafr El-Sheikh, Egypt: implications for human health. *Environ Sci Pollut Res* 28:2007–2018
- Jiang Y, Shi L, Guang A, Mu Z, Zhan H, Wu Y (2018) Contamination levels and human health risk assessment of toxic heavy

- metals in street dust in an industrial city in Northwest China. *Environ Geochem Health* 40(5):2007–2020
- Jiang W, Meng L, Liu F, Sheng Y, Chen S, Yang J, Mao H, Zhang J, Zhang Z, Ning H (2023) Distribution, source investigation, and risk assessment of topsoil heavy metals in areas with intensive anthropogenic activities using the positive matrix factorization (PMF) model coupled with self-organizing map (SOM). *Environ Geochem Health* 45(8):6353–6370
- Kierczak J, Pietranik A, Pędziwiatr A (2021) Ultramafic geoecosystems as a natural source of Ni, Cr, and Co to the environment: a review. *Sci Total Environ* 755:1–18
- Masto R, George J, Rout T, Ram L (2017) Multi element exposure risk from soil and dust in a coal industrial area. *J Geochem Explor* 176:100–107
- Miletić A, Lučić M, Onjia A (2023) Exposure factors in health risk assessment of heavy metal(loid)s in soil and sediment. *Metals* 13(7):1–28
- Nimyel SH, Namadi MM (2020) Assessment of the level of heavy metal concentration in the street dust in some selected locations in Zaria metropolis, Kaduna state. *Nigeria Fudma J Sci* 4(3):93–98
- OG (Official Gazette) (2005). Soil pollution control regulation (Republic of Turkey Ministry of Environment and Forestry). p 25831, 31 Mayıs 2005 (in Turkish)
- R Core Team R (2023) A language and environment for statistical computing. R Foundation for Statistical Computing, Vienna
- Riaz MH, Khitab A, Ahmed S (2019) Evaluation of sustainable clay bricks incorporating Brick Kiln Dust. *J Build Eng* 24:1–8
- Sabouhi M, Ali-Taleshi MS, Bourliva A, Nejadkoorki F, Squizzato S (2020) Insights into the anthropogenic load and occupational health risk of heavy metals in floor dust of selected workplaces in an industrial city of Iran. *Sci Total Environ* 744:1–13
- Saha A, Zakir HM, Quadir QF, Sarker N, Biswas P, Mallick S (2024) Human health risks of trace metals through the dietary intake of potato tubers and exposures of potato cultivating soils: a case study of Mymensingh district, Bangladesh. *J Trace Elem Min* 8:1–14
- Sarmadi M, Rahimi S, Rezaei M, Sanaei D, Dianatinasab M (2021) Air quality index variation before and after the onset of COVID-19 pandemic: a comprehensive study on 87 capital, industrial and polluted cities of the world. *Environ Sci Eur* 33(134):1–17
- Sood H, Gupta G, Gupta PK (2021) Application of brick kiln dust for sustainable construction. In: Singh H, Singh Cheema PP, Garg P (eds) Sustainable development through engineering innovations, vol 113. Springer, Singapore
- Sultana Z, Rehman MYA, Khan HK, Malik RN (2023) Health risk assessment associated with heavy metals through fractionated dust from coal and chromite mines in Pakistan. *Environ Geochem Health* 45:1617–1633
- Suryawanshi PV, Rajaram BS, Bhanarkar AD, Chalapati Rao CV (2016) Determining heavy metal contamination of road dust in Delhi. *India Atmósfera* 29(3):221–234
- Tan SY, Praveena SM, Abidin EZ, Cheema MS (2016) A review of heavy metals in indoor dust and its human health-risk implications. *Rev Environ Health* 31(4):447–456
- Tang Z, Chai M, Cheng J, Jin J, Yang Y, Nie Z, Huang Q, Li Y (2017) Contamination and health risks of heavy metals in street dust from a coal-mining city in Eastern China. *Ecotoxicol Environ Saf* 138:83–91
- Thygeson SM, Sanjel S, Johnson S (2016) Occupational and environmental health hazards in the brick manufacturing industry in Kathmandu Valley. *Nepal Occup Med Health Aff* 4(5):1–7
- Tong R, Cheng M, Yang X, Yang Y, Shi M (2019) Exposure levels and health damage assessment of dust in a coal mine of Shanxi Province, China. *Process Saf Environ Prot* 128:184–192
- Torres P, Llopis AL, Melo CS, Rodrigues A (2023) Environmental impact of cadmium in a volcanic archipelago: research challenges related to a natural pollution source. *J Mar Sci Eng* 11(1):1–18
- TUIK (Turkish Statistical Institute) (2024). Web page: <https://data.tuik.gov.tr/Bulten/Index?p=Life-Tables-2020-2022-49726>
- Turhan Ş, Garad AMK, Hañçerlioğulları A, Kurnaz A, Gören E, Duran C, Karataşlı M, Altukulaç A, Savacı G, Aydın A (2020) Ecological assessment of heavy metals in soil around a coal-fired thermal power plant in Turkey. *Environ Earth Sci* 79(134):1–15
- Turhan Ş, Turfan N, Kurnaz A (2023) Heavy metal contamination and health risk evaluation of chestnut (*Castanea sativa* Miller) consumed in Turkey. *Int J Environ Health Res* 33(11):1091–1101
- USEPA (United States Environmental Protection Agency) (1989) Risk assessment guidance for superfund. Volume I: Human health evaluation manual (Part A), EPA/540/1–89/002, Washington
- USEPA (United States Environmental Protection Agency) (2004) Risk assessment guidance for superfund. Volume 1: Human health evaluation manual (Part E, Supplemental Guidance for Dermal Risk Assessment). EPA/540/R/99/005, Office of superfund remediation and technology innovation, US Environmental Protection Agency Washington
- USEPA (United States Environmental Protection Agency) (2011) Soil and dust ingestion. Exposure factors handbook (Final Report). US Environmental Protection Agency, Washington, p 2011
- USEPA (United States Environmental Protection Agency) (2014a) Regional screening levels (RSLs)-Generic tables (May 2016). US Environmental Protection Agency, Washington, p 2011
- USEPA (United States Environmental Protection Agency) (2014b) EPA positive matrix factorization (PMF) 5.0 fundamentals and user guide. US Environment Protection Agency, Washington, p 2014
- Vaezi A, Shahbazi R, Lak R, Ahmadi N, Sheikh M, Gol ARM (2023) Assessment of potentially toxic elements in atmospheric dust and associated health risks in Zahedan City. *Iran Environ Geochem Health* 45(11):7759–7773
- Wang Y, Xu J, Liu G (2023) Characteristics and health risk assessment of heavy metals in dust of a waste printed circuit board recycling workshop. *China RSC Adv* 3(32):22216–22225
- Xu Z, Mi W, Mi N, Fan X, Tian Y, Zhou Y, Zhao Y-N (2021) Heavy metal pollution characteristics and health risk assessment of dust fall related to industrial activities in desert steppes. *PeerJ* 9:1–26
- Yaroshevsky AA (2006) Abundances of chemical elements in the Earth's crust. *Geochem Int* 44(1):48–55
- Yoon S, Kim DM, Yu S, Batsaikhan B, Kim T, Yun ST (2023) Characteristics of soil contamination by potentially toxic elements in mine areas of Mongolia. *Environ Geochem Health* 46(1):1–18
- Zhang X, Wei S, Sun Q, Wadood SA, Guo B (2018) Source identification and spatial distribution of arsenic and heavy metals in agricultural soil around Hunan industrial estate by positive matrix factorization model, principle components analysis and geo statistical analysis. *Ecotoxicol Environ Saf* 159:354–362

**Publisher's Note** Springer Nature remains neutral with regard to jurisdictional claims in published maps and institutional affiliations.